

Driven disordered periodic media with an underlying structural phase transition

Ankush Sengupta and Surajit Sengupta

Satyendra Nath Bose National Centre for Basic Sciences, Block-JD, Sector-III, Salt Lake, Kolkata 700 098, India

Gautam I. Menon

The Institute of Mathematical Sciences, CIT Campus, Taramani, Chennai 600 113, India

(Received 16 April 2007; published 10 May 2007)

We study the nonequilibrium steady states of a crystal whose ground state can be tuned through a square-triangular transition. Driving such a system across a quenched random background yields a complex sequence of dynamical states. These include plastic flow states, anisotropic hexatics, dynamically stabilized triangle and square phases, and intermediate regimes of phase coexistence with anomalously slow dynamics. Such states should be observable in transport experiments on the mixed phase of several superconductors which exhibit related structural transitions. They may also be accessible in similar experiments on adsorbed monolayer colloids with tunable interactions.

DOI: 10.1103/PhysRevB.75.180201

PACS number(s): 64.60.-i, 61.43.-j, 74.25.Qt, 83.80.Hj

When driven far from equilibrium, condensed matter systems often exhibit a far more varied set of phases than their equilibrium counterparts. The understanding of such phases and transitions between them is central to the physics of nonequilibrium steady states.¹ A variety of such states are obtained in the depinning and flow of randomly pinned, *periodic* media, such as charge-density-wave systems and Abrikosov flux-line lattices in the mixed state of type-II superconductors.² Many such superconductors exhibit structural transitions in the mixed state, typically between flux-line lattices with triangular and rectangular symmetry.³ Colloidal systems such as poly(methyl methacrylate) spheres coated with a low-molecular-weight polymer undergo a remarkable variety of solid-solid transformations in an external field.⁴ While applying a sufficiently large current depins the flux lines from the quenched random disorder present in all real materials, the possibility of driving colloidal particles in two dimensions across a disordered substrate has also been raised.⁵ What links these diverse systems is the generic problem of understanding the competition between an underlying structural phase transition in a pure periodic system as modified by disorder, and the nonequilibrium effects of an external drive. This Rapid Communication proposes and studies a simple model that describes this physics.

Our model system is two dimensional and consists of particles with two- and three-body interactions.⁶ The three-body interaction, parametrized through a single parameter v_3 , tunes the system across a square-triangular phase transition. Our central result, the sequence of steady states obtained as a function of increasing force for various values of v_3 , is summarized in the dynamical “phase” diagram of Fig. 1. We obtain a variety of phases: pinned states which may have dominantly triangular or square correlations, a moving liquid or glass phase, a moving anisotropic hexatic glass phase, flowing triangular and square states ordered over the size of our simulation cell, and a dynamic coexistence regime between these ordered phases. We discuss our characterization of these states and the applicability of simple dynamical criteria for nonequilibrium phase transitions between them.

The model. Particles interact in two dimensions through the interaction potential $(1/2)\sum_{i\neq j}V_2(r_{ij}) + (1/6)\sum_{i\neq j\neq k}V_3(r_i, r_j, r_k)$, where \mathbf{r}_i is the position vector of

particle i , $r_{ij} \equiv |\mathbf{r}_{ij}| \equiv |\mathbf{r}_j - \mathbf{r}_i|$, $V_2(r_{ij}) = v_2(\sigma_0/r_{ij})^{12}$, and $V_3(r_i, r_j, r_k) = v_3[f_{ij}\sin^2(4\theta_{ijk})f_{jk} + (\text{permutations})]$.⁶ The function $f_{ij} \equiv f(r_{ij}) = (r_{ij} - r_0)^2$ for $r_{ij} < 1.8\sigma_0$ and 0 otherwise, and θ_{ijk} is the angle between \mathbf{r}_{ji} and \mathbf{r}_{jk} . The two-body (three-body) interaction favors a triangular (square) ground state. Energy and length scales are set using $v_2 = 1$ and $\sigma_0 = 1$. Particles also interact with a quenched random background modeled as a Gaussian random potential⁷ $V_d(\mathbf{r})$ with zero mean and exponentially decaying (short-range) correlations. The disorder variance is set to $v_d^2 = 1$ and its spatial correlation length is $\xi = 0.12$. The system evolves through standard Langevin dynamics $\dot{\mathbf{r}}_i = \mathbf{v}_i$ and $\dot{\mathbf{v}}_i = \mathbf{f}_i^{\text{int}} - \alpha \mathbf{v}_i + \mathbf{F} + \boldsymbol{\eta}_i(t)$. Here \mathbf{v}_i

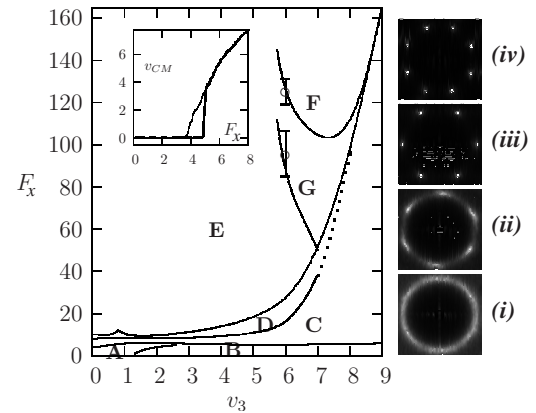


FIG. 1. Dynamical phase diagram in the v_3 - F_x plane. The phases are A, pinned triangle, B, pinned square, C, plastic flow or isotropic liquid, D, driven hexatic glass, E, moving triangle, F, moving square, and G, dynamical square-triangle coexistence. Two points with error bars show the boundary of G for $v_3=6$, obtained by averaging over 24 disorder realizations, as an example. The boundaries for all other transitions are considerably sharper. The inset shows the center of mass velocity $v_{c.m.}$ as a function of the driving force F_x as the force is increased (bold) and then decreased across the depinning transition. The right panel shows $S(\mathbf{q})$ for the plastic flow state (i), driven hexatic glass (ii), moving triangle (iii), and moving square solid phases (iv) at $v_3=6.0$ and $F_x=10, 20, 60$, and 140, respectively. To obtain $S(\mathbf{q})$, 50 independent configurations were used. The structure in (iv) reflects the presence of two mutually misoriented square crystallites.

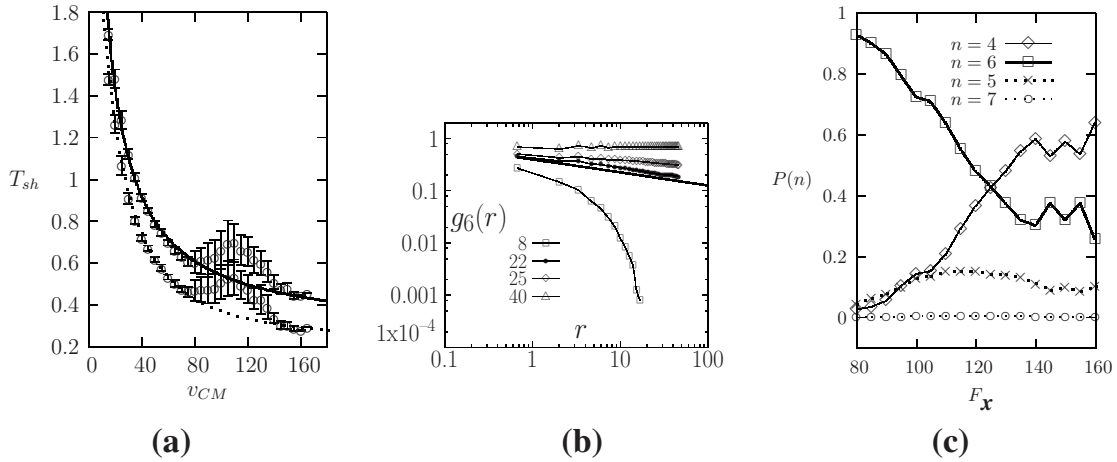


FIG. 2. (a) Shaking temperatures for a system with $v_3=6$ as a function of F_x in the drive (x) and transverse (y) directions. These are obtained by averaging over 100 independent configurations as well as over 25 separate disorder realizations. For F_x in the coexistence region, there is a significant enhancement of the shaking temperature in excess of the prediction of KV (Ref. 9). The lines represent fits to the KV form. (b) Hexatic correlation function $g_6(r)$ for $F_x=8, 22, 25$, and 40 , each averaged over 50 independent configurations of a 10 000-particle system at $v_3=6$. The solid line indicates the universal behavior $g_6(r) \sim r^{-1/4}$ at the liquid to hexatic transition. (c) $P(n)$ for $n=4, 5, 6, 7$ (see text) vs F_x averaged as in (a).

is the velocity, $\mathbf{f}_i^{\text{int}}$ the total interaction force, and $\eta_i(t)$ the random force acting on particle i . A constant force $\mathbf{F} = \{F_x, 0\}$ drives the system and the zero-mean thermal noise $\eta_i(t)$ is specified by $\langle \eta_i(t) \eta_j(t') \rangle = 2T \delta_{ij} \delta(t-t')$ with $T=0.1$, well below the equilibrium melting temperature of the system. The unit of time $\tau = \alpha \sigma_0^2 / v_2$, with $\alpha=1$ the viscosity.

Simulation details. Our system consists of 1600 particles in a square box at number density $\rho=1.1$. At $T=0.1$, the pure system remains triangular up to $v_3=1.5$. For larger v_3 , a square phase is obtained. Larkin length estimates² yield $L_a/a \sim 100$, with $a=1/\rho^{1/2}$ the lattice parameter, somewhat larger than our system size.

Configurations obtained through a simulated annealing procedure are the initial inputs to our Langevin simulations. We evolve the system using a time step of $10^{-4}\tau$. The external force F_x is ramped up from a starting value of 0, with the system maintained at up to 10^8 steps at each F_x .

Observables. We monitor structural observables, such as the static structure factor $S(\mathbf{q}) = \sum_{ij} \exp(-i\mathbf{q} \cdot \mathbf{r}_{ij})$. Delaunay triangulations yield the probability distributions $P(n)$ of $n=4, 5, 6$, and 7 coordinated particles [$\sum_n P(n)=1$].⁸ We define order parameters $\psi = [P(4) - P(6)] / [P(4) + P(6)]$ to distinguish between square and triangular phases, $\psi_\Delta = [P(6) - P(5) - P(7)] / [P(6) + P(5) + P(7)]$ to distinguish between liquid (disordered) and triangular crystals, and $\psi_\square = [P(4) - P(5) - P(7)] / [P(4) + P(5) + P(7)]$ to distinguish between liquid and square crystals. In addition, we compute the hexatic order parameter $\psi_6 = \sum_{ij} \exp(-i6\theta_{ij})$ and its correlations, where θ is the bond angle measured with respect to an arbitrary external axis. The dynamical variables we study include the center of mass velocity $v_{c.m.}$ and the particle flux and its statistics. As suggested in a proposal due to Koshelev and Vinokur (KV),⁹ it is often useful to think of the combination of the drive and the disorder as yielding an effective “shaking” temperature in the moving phase, as measured through transverse and longitudinal fluctuations of the velocity. We calculate the KV shaking temperature⁹ T_{sh}^ν appropri-

ate to the drive and transverse directions, obtaining it from

$$T_{sh}^\nu = \langle [v^\nu - v_{c.m.}^\nu]^2 \rangle / 2, \quad \nu = x, y.$$

For small F_x the solid is pinned. A disorder-broadened version of the equilibrium triangle (A) to square (B) transition results as v_3 is varied across the $T=0$ transition value at small F_x ; here and below, letters in parentheses refer to the states labeled in Fig. 1. The triangular (A) phase is favored at nonzero F_x . Upon further increasing F_x , the system undergoes a *discontinuous* depinning transition which exhibits prominent hysteresis behavior (Fig. 1, inset). Such a depinned state is inhomogeneous and undergoes plastic flow^{10–15} consistent with earlier numerical work. For larger F_x the velocity approaches the asymptotic behavior $v_{c.m.} = F_x$.

The structure factor $S(q)$ of the plastically moving phase (C) obtained just above the depinning transition consists of liquidlike isotropic rings [Fig. 1(i)]. Upon increasing F_x , the circular ring in $S(q)$ concentrates into six smeared peaks which we associate with a hexatic glass (D).¹⁶ Unlike the hexatic phase obtained in a pure, nondriven system, the driven hexatic glass is strongly anisotropic, with the hexatic director aligning itself with the drive direction. Figure 2(b) shows the evolution of the hexatic correlation function $g_6(r) = \langle \psi_6(0) \psi_6(r) \rangle$, as F_x is varied across (C) \rightarrow (D) \rightarrow (E). Note the sharp exponential decay of hexatic correlations in (C). In (D) and (E), the orientational correlation function asymptotically saturates, as expected, to a constant ($\sim F_x^2$); in (D), such saturation is obtained only in the drive direction. The transition from (D) to (E), when triangular *translational* order increases continuously with F_x , is smooth.

The plastic flow regime (C), as well as that of the hexatic glass (D) expands at larger v_3 ,¹⁷ due to the frustration of local triangular translational order by three-body effects. On further increasing F_x , the structure obtained depends on the value of v_3 : for low v_3 the final crystal is triangular (E)

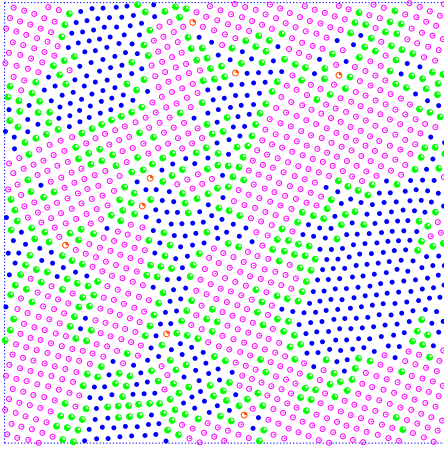


FIG. 3. (Color online) Single particle configuration showing square-triangle coexistence at $F_x=107$. The particles are colored according to the number of neighbors computed from the Delaunay mesh $n=4$ [magenta (open) circle], 5 [green (filled gray) circle with white spot], 6 [blue (filled gray) circle], and 7 [orange (open) circle with black spot]. Particles with coordination 5 are present mainly in the interfacial region while those with 7 are associated with isolated dislocations.

whereas for large v_3 it is square (F). For intermediate v_3 the system first freezes into a triangular structure but subsequently transforms into the square via an intervening “coexistence” regime (G) best described as a mosaic of dynamically fluctuating square and triangular regions.

The phase diagram of the pure system in thermal equilibrium accommodates fluid, triangular solid, and square solid phases.⁶ In the driven system, as F_x is increased, analogous phases appear in approximately the inverse order to the sequence obtained in the pure case as T is increased. Our observations agree qualitatively with the KV proposal if the shaking temperature T_{sh} is identified with T . The shaking temperatures are predicted to fall as $\sim 1/v^2$ and as $\sim 1/v$ in the drive and the transverse directions, respectively, consistent with our observations in Fig. 2(a). We find that T_{sh}^v is nearly independent of v_3 . Importantly, within the putative

coexistence regime, T_{sh}^v behaves nonmonotonically, implying a breakdown of the KV prediction [see Fig. 2(a)]. Typically, for a particular disorder configuration and for $5.5 < v_3 < 8.5$, T_{sh}^v appears to increase sharply at a well-defined F_x , signifying the start of coexistence. Within G , T_{sh}^v remains high but drops sharply at the upper limit of G , to continue to follow the interrupted KV behavior. The limits of the coexistence region, though sharp for any typical disorder realization, vary considerably between realizations.

Within the coexistence region the probability of obtaining triangular (square) regions appears to decrease (increase) roughly linearly with F_x ; see Fig. 2(c). Real space configurations (Fig. 3) exhibit islands of square and triangular coordination connected by interfacial regions with predominantly five-coordinated particles. Particles with coordination 7 are typically associated with dislocations, which are scattered randomly in the interface. This configuration, in the comoving frame, is extremely dynamic, with the islands rapidly interconverting between square and triangle. This interconversion has complex temporal properties: the power spectrum of coordination number fluctuations shows a prominent $1/f$ falloff over several decades. In addition, particle current fluctuations are enhanced by an order of magnitude, also displaying a regime of $1/f$ behavior (Fig. 4), although over a restricted range as a consequence of the proximity to the washboard frequency. This anomalous enhancement of fluctuation magnitudes provides strong evidence for a genuine coexistence phase, since increasing the driving force would be expected to reduce current noise monotonically once the system depins, as observed in all previous simulation work on related models.^{12–14}

Renormalization group arguments suggest that neither translational long-range order nor quasi-long-range order survives in the disordered moving state in two dimensions at any finite drive,^{18–20} the closest analog of the crystalline state in the undriven pure system being the moving Bragg glass state argued to be stable in three dimensions and higher.²⁰ The ordered square (F) and triangular (E) states we obtain at large drives are then to be understood as a finite-size effect arising from the restricted size of our simulation box, al-

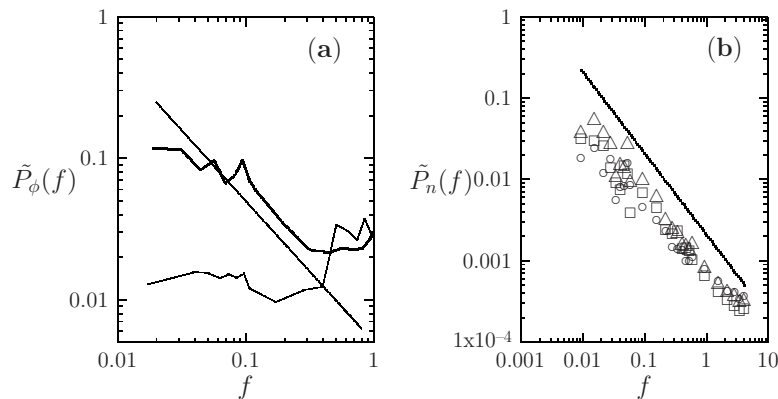


FIG. 4. (a) Power spectrum $\tilde{P}_\phi(f)$ of current fluctuations in the moving triangle phase (thin line, $F_x=55$) and in the coexistence region (bold line, $F_x=100$), logarithmically binned and plotted for a range of frequencies below the washboard frequency. Current fluctuations in the coexistence region are enhanced, also showing a $1/f$ decay at intermediate frequencies. (b) $\tilde{P}_n(f)$ for the fluctuations of the numbers of four- (\square) , five- (\circ) , and six- (\triangle) coordinated particles in the coexistence region. The number of seven-coordinated particles (not shown) is vanishingly small. The straight line in both figures represents the $1/f$ law.

though the crossover length scales can be very large at weak disorder.^{18,20} The possibility of alternative dynamically stabilized states with reduced levels of ordering, such as driven transverse smectics, is attractive.^{18,21} In contrast to some previous work,^{11,13,14} we see no evidence for smectic order and flow in weakly coupled channels at large drives—our channels always remain strongly coupled—but note that moving states in which channels transverse to the drive direction are effectively decoupled may be stabilized at higher levels of thermal noise or randomness.¹⁴

The coexistence state appears to be a genuine nonequilibrium state, separated from other regimes through sharp nonequilibrium transitions. Theoretical work has, so far, neglected the possibility of such dynamic phase coexistence in the nonequilibrium steady states of driven disordered crystals.²¹ A nondisordered but frustrated system closely related to the one considered here has been proposed recently as a model for the dynamical heterogeneity seen in the glassy state.²² In this model, fluctuating regions of crystalline ordering within a liquid background are argued to be responsible for the anomalous dynamical behavior and slow relaxation in the glassy state, a physical picture which shares some similarities to our ideas regarding the coexistence regime.

We now summarize the central results of this Rapid Communication, augmenting the phase diagram of Fig. 1. These results are (a) the drive-induced stabilization of the triangular lattice state even well into regimes where v_3 would favor a square; (b) the demonstration of a distinct coexistence regime in a narrow and reproducible regime in parameter

space; (c) the observation of a variety of dynamical anomalies within the coexistence regime including enhanced noise signals with $1/f$ character; and (d) the expansion of the plastic flow regime at large v_3 . Thus, the competition between structural phase transitions in a pure system as modified by disorder, coupled to the nonequilibrium effects of an external drive, is demonstrated to have a variety of nontrivial and previously unanticipated consequences.

The three-body interaction strengths we consider here are physically accessible, as borne out by recent experimental measurements on two-dimensional colloidal systems, which find the magnitude of the three-body term to be comparable to the term arising from the pair interaction at the mean interparticle separation.²³ The ubiquity of structural phase transitions in the vortex state of a large number of superconductors which have been studied recently, as well as the relative ease with which the vortex state can be driven, suggests experimental situations in which the ideas here should find application. Functionalized colloidal particles driven over random substrates constitute a system on which our proposals can be tested.^{5,24} Such systems have the further advantage that interparticle interactions can be tuned both through surface modifications and through the application of external fields.²⁴

The authors thank M. Rao, A. Chaudhuri, C. Dasgupta, and A. van Blaaderen for discussions and acknowledge the DST (India) for financial support.

¹Nonequilibrium Statistical Systems, edited by M. Barma, special issue of Curr. Sci. **77**, 402 (1999).

²T. Giamarchi and S. Bhattacharya, in *High Magnetic Fields: Applications in Condensed Matter Physics and Spectroscopy*, edited by C. Berthier, L. P. Levy, and G. Martinez (Springer-Verlag, Berlin, 2002), p. 314.

³C. D. Dewhurst, S. J. Levett, and D. McK. Paul, Phys. Rev. B **72**, 014542 (2005); L. Ya. Vinnikov, T. L. Barkov, P. C. Canfield, S. L. Budko, J. E. Ostenson, F. D. Laabs, and V. G. Kogan, *ibid.* **64**, 220508(R) (2001); B. Rosenstein, B. Ya. Shapiro, I. Shapiro, Y. Bruckental, A. Shaulov, and Y. Yeshurun, *ibid.* **72**, 144512 (2005); S. P. Brown, D. Charalambous, E. C. Jones, E. M. Forgan, P. G. Kealey, A. Erb, and J. Kohlbrecher, Phys. Rev. Lett. **92**, 067004 (2004); R. Gilardi, J. Mesot, S. P. Brown, E. M. Forgan, A. Drew, S. L. Lee, R. Cubitt, C. D. Dewhurst, T. Uefuji, and K. Yamada, *ibid.* **93**, 217001 (2004).

⁴A. Yethiraj and A. van Blaaderen, Nature (London) **421**, 513 (2003); A. Yethiraj, Alan Wouterse, Benito Groh, and Alfons van Blaaderen, Phys. Rev. Lett. **92**, 058301 (2004).

⁵A. Pertsinidis and X. S. Ling, Bull. Am. Phys. Soc. **46**, 181 (2001); **47**, 440 (2002); C. Reichhardt and C. J. Olson, Phys. Rev. Lett. **89**, 078301 (2002).

⁶M. Rao and S. Sengupta, J. Phys.: Condens. Matter **16**, 7733 (2004); Phys. Rev. Lett. **91**, 045502 (2003).

⁷E. M. Chudnovsky and R. Dickman, Phys. Rev. B **57**, 2724 (1998); A. Sengupta, S. Sengupta, and G. I. Menon, Europhys. Lett. **70**, 635 (2005).

⁸F. R. Preparata and M. I. Shamos, *Computational Geometry: An Introduction* (Springer-Verlag, New York, 1985).

⁹A. E. Koshelev and V. M. Vinokur, Phys. Rev. Lett. **73**, 3580 (1994); S. Scheidl and V. M. Vinokur, Phys. Rev. B **57**, 13800 (1998).

¹⁰H. J. Jensen, A. Brass, and A. J. Berlinsky, Phys. Rev. Lett. **60**, 1676 (1988).

¹¹K. Moon, R. T. Scalettar, and G. T. Zimanyi, Phys. Rev. Lett. **77**, 2778 (1996).

¹²M. C. Faleski, M. C. Marchetti, and A. A. Middleton, Phys. Rev. B **54**, 12427 (1996).

¹³C. J. Olson, C. Reichhardt, and F. Nori, Phys. Rev. Lett. **81**, 3757 (1998).

¹⁴H. Fangohr, S. J. Cox, and P. A. J. de Groot, Phys. Rev. B **64**, 064505 (2001).

¹⁵M. Chandran, R. T. Scalettar, and G. T. Zimanyi, Phys. Rev. B **67**, 052507 (2003).

¹⁶S. Ryu, A. Kapitulnik, and S. Doniach, Phys. Rev. Lett. **77**, 2300 (1996).

¹⁷Although the plastic flow regime expands as v_3 is increased over the scales shown in Fig. 1, it collapses at much larger $v_3 \approx 30$ (not shown).

¹⁸L. Balents, M. C. Marchetti, and L. Radzihovsky, Phys. Rev. Lett. **78**, 751 (1997); Phys. Rev. B **57**, 7705 (1998).

¹⁹S. Scheidl and V. M. Vinokur, Phys. Rev. E **57**, 2574 (1998).

²⁰P. LeDoussal and T. Giamarchi, Phys. Rev. B **57**, 11356 (1998).

²¹T. Nattermann and S. Scheidl, Adv. Phys. **49**, 607 (2000).

²²H. Shintani and H. Tanaka, Nat. Phys. **2**, 200 (2006).

²³M. Brunner, J. Dobnikar, H-H. von Grunberg, and C. Bechinger, Phys. Rev. Lett. **92**, 078301 (2004).

²⁴A. van Blaaderen, Nature (London) **439**, 545 (2006).